PISTORIUS, P.C. Equilibrium interactions between freeze lining and slag in ilmenite smelting. *VII International Conference on Molten Slags Fluxes and Salts,* The South African Institute of Mining and Metallurgy, 2004.

Equilibrium interactions between freeze lining and slag in ilmenite smelting

P. C. PISTORIUS

Department of Materials Science and Metallurgical Engineering, University of Pretoria, Pretoria, South Africa

In ilmenite smelting, the FeO content of the feed material (nominally $FeO.TiO_2$) is decreased by reduction with carbon. In a parallel reaction, a significant amount of the TiO_2 is reduced to Ti_2O_3. One of the striking features of these reactions is a consistent relationship between the extents of FeO and TiO_2 reduction; this relationship is independent of furnace size. It was recently proposed that this relationship follows from the solidification behaviour of the slag, where the final slag composition corresponds to the minimum melting point ('eutectic groove') in the $FeO\text{-}TiO_2\text{-}Ti_2O_3$ phase system; the hypothesis is that solidification equilibrium with the freeze lining stabilizes the slag composition. If this is the case, the system of slag and freeze lining must be capable of correcting two types of disturbances: thermal and compositional. Thermal disturbances result from incorrect power input, for the feed rates of ilmenite and reductant. For example, excessive power input will tend to overheat the slag, causing the freeze lining to melt partially, establishing a new steady-state heat loss from the furnace. Compositional disturbances result from an incorrect reductant input for the given power and ilmenite input.

In this work, the dynamic response of the slag and freeze lining to different inputs (flow rates of ilmenite and reductant, and power input) is modelled. The model is based on solidification equilibria, and quantified heat loss through the freeze lining. The conclusion is that the solidification equilibrium cannot constrain the composition to the eutectic groove for typical operating conditions.

Keywords: ilmenite smelting, freeze lining, solidification, high-titanium slag

Background

Ilmenite smelting is one of the methods to upgrade the iron-titanium oxide mineral ilmenite to a high-titanium feedstock for rutile pigment manufacture. The product of ilmenite smelting is a high-titanium slag, which typically contains around 9% FeO, 50% TiO_2, and 35% Ti_2O_3, with the balance being other impurity oxides. This slag is corrosive to refractory materials, and hence a layer of solidified slag is used as a 'freeze lining' on the furnace sidewalls.

The freeze lining hence plays an essential role in protecting the furnace lining. It has recently been suggested that the interplay between the solidified freeze lining and the liquid slag also affects the composition of the liquid slag[1]: a line of minimum melting points (a 'eutectic groove') was found to separate the primary phase fields of rutile (TiO_2) and pseudobrookite (M_3O_5, a solid-solution phase, which is a combination of $FeTi_2O_5$ and Ti_3O_5 in the three-component system $FeO\text{-}TiO_2\text{-}Ti_2O_3$). It was suggested that the solidification equilibrium forces the liquid slag composition to lie along the eutectic groove.

This suggestion offers a possible explanation for the remarkable constancy of the phase composition of solidified titania slag (this constancy is that solidified slag mainly consists of M_3O_5 and a few per cent of rutile,[2] with the minor components SiO_2 and CaO in separate phases; the dominance of the M_3O_5 phase persists over a wide range of FeO contents). As Figure 1 indicates, the eutectic groove

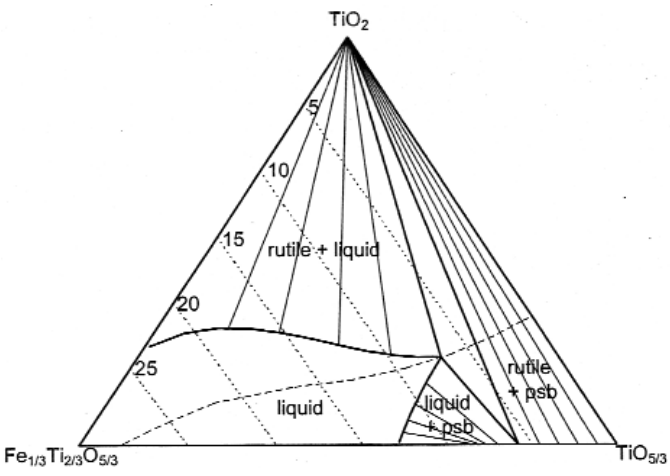

Figure 1. Isothermal section through part of the TiO_2-FeO-Ti_2O_3 system, at 1875 K. The base of the diagram represents the M_3O_5 solid solutions, between ferrous pseudobrookite (here shown as $Fe_{1/3}Ti_{2/3}O_{5/3}$) and anosovite (shown as $TiO_{5/3}$). Diagonal broken lines indicate compositions of constant FeO content, on a mass basis, of respectively 5, 10, 15, 20 and 25%. Some tie lines are shown in the dual-phase regions. The curved broken line from lower left to right is the 'eutectic groove' which separates the rutile and pseudobrookite primary phase fields. Diagram calculated on the basis of curve-fits to equilibrium data taken from FACTSage

Table I
Coefficients in enthalpy expressions used in energy balance equations; expressions are of the form $H° = a + bT + cT^2$, where T is the temperature in kelvin, and $H°$ is the standard enthalpy in J/mol

Species	*a*	*b*	*c*
TiO_2	- 966 532	67.85	0.002844
Ti_3O_5	- 2 495 862	159.0	0.02511
$FeTi_2O_5$	- 2 212 171	184.1	0.01140

Table II
Enthalpy expression for liquid slag. Expression is of the form $H_{slag} = \sum_i d_i X_i + e(T - 2023)$, where X_i is the mole fraction of each species in the slag (here taken to be FeO, $TiO_{1.5}$ and TiO_2), d_i is the coefficient for each species, e is the heat capacity, T is the temperature in kelvin, and H_{slag} is the slag enthalpy in kJ/g-atom.

Constant	$d_{TiO_{1.5}}$	d_{FeO}	d_{TiO_2}	*e*
Value	-236.3	-106.8	-257	0.0275
Units	kJ/g-atom	kJ/g-atom	kJ/g-atom	kJ/g-atom.K

lies between the M_3O_5 and rutile compositions, which means that slags with compositions along the groove solidify as a mixture of M_3O_5 and rutile. (The predicted phase diagram does indicate a larger fraction of rutile in solidified slags than found in practice–for example, a slag with 10% FeO [mass basis] and which lies on the eutectic groove, is predicted to contain 18% rutile after solidification, about 3 times the actual amount.)

In the work presented here, the suggestion–that interaction with the freeze lining serves to stabilise the slag composition along the eutectic groove–is tested by using solidification equilibrium data (ternary phase diagrams for the FeO-TiO_2-Ti_2O_3 system), and a simple heat transfer model. This model was used to test the sensitivity of the slag composition to thermal and compositional perturbations.

In the following section, the relevant equilibrium data are summarized first; the model description and model results then follow.

Equilibrium data

Calculation procedure

The phase diagram data were calculated by using the FACTSage[3] software, using the quasichemical model for the liquid slag and near-ideal solid solution in M_3O_5 as described before,[4] and considering rutile as pure TiO_2 (i.e. neglecting the small solubility of Ti_2O_3 in rutile). Magnéli phases were also not considered, for the reason that solidified slag has not been found to contain these phases (although thermodynamic calculations indicate that they should form). Compositions lying between M_3O_5 and TiO_2 were considered, since this is the range of actual tap compositions. In the phase diagrams shown in Figure 1 and later figures, the end species are taken as TiO_2 (rutile), $Fe_{1/3}Ti_{2/3}O_{5/3}$ (ferrous pseudobrookite, normally written as $FeTi_2O_5$, but shown here as the species containing 1 cation per formula unit), and $TiO_{5/3}$ (anosovite, normally written as Ti_3O_5). (For the single-cation forms of the end species chosen here, mole fractions are nearly equal to mass percentages.)

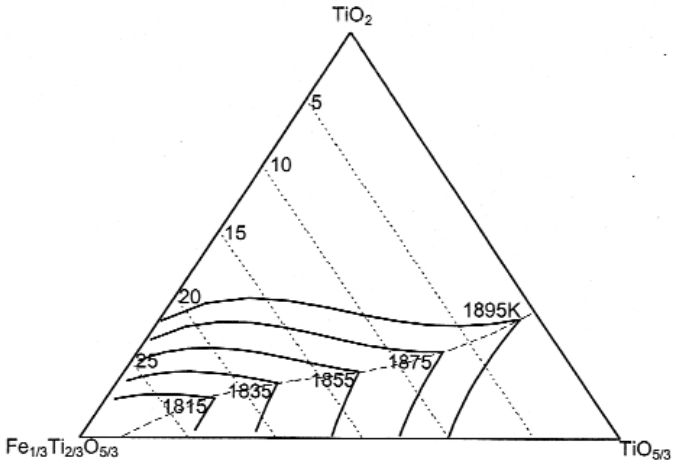

Figure 2. Extent of fully liquid region in the TiO_2- $Fe_{1/3}Ti_{2/3}O_{5/3}$-$TiO_{5/3}$ system, for temperatures from 1815 K to 1895 K. Diagonal broken lines indicate compositions of constant FeO content, on a mass basis, of respectively 5, 10, 15, 20 and 25%. The curved broken line from lower left to right is the 'eutectic groove' which separates the rutile and pseudobrookite primary phase fields. Diagram calculated on the basis of curve-fits to equilibrium data taken from FACTSage

For speed of calculation in the heat transfer model, the phase equilibrium data generated with FACTSage were represented by a series of polynomial expressions, which describe the shapes of the liquid/(rutile+liquid) phase boundary and the liquid/(pseudobrookite+liquid) phase boundary, and the dependence of the slopes of the pseudobrookite-liquid tie lines on pseudobrookite composition. Different polynomials were fitted to phase boundaries for temperatures from 1815 K to 1895 K, at intervals of 10 K; as Figure 2 indicates, the range from 1815 K to 1895 K spans the liquidus temperatures of slags which lie along the eutectic groove, with FeO contents ranging from as little as 1.5% to 22%.

With these data on phase equilibria, a program was written (in Visual Basic) to calculate the equilibrium phase composition (amounts of phases, and composition of each phase, at a given temperature and overall composition), for slags in the TiO_2-$Fe_{1/3}Ti_{2/3}O_{5/3}$-$TiO_{5/3}$ system. The enthalpy of the phase mixture was found by assuming the $Fe_{1/3}Ti_{2/3}O_{5/3}$-$TiO_{5/3}$ (pseudobrookite) solid solution to be ideal, and using heats of solution for the liquid slag as deduced from the quasichemical model. Simplified expressions were fitted to the enthalpy data; these expressions are listed in Tables I and II.

Solidification behaviour: heat of solidification and solidification range

Two prominent features of solidification in this system are worth emphasizing; these features have strong effects on the freeze lining behaviour. These two features are the narrow solidification range, and the large heat of solidification compared with the heat capacity of the liquid and solid phases; both features are illustrated by Figure 3 (a) and (b). This figure plots the calculated enthalpy of three mixtures which contain 10% FeO by mass, but which lie at different locations relative to the eutectic groove–to give respectively rutile, pseudobrookite, and a combination of both, as primary phases. Note that the enthalpy values are given in joule per g-atom,[5] where 'g-atom' indicates the number of moles of *atoms* (Fe, Ti and O) in the mixture.

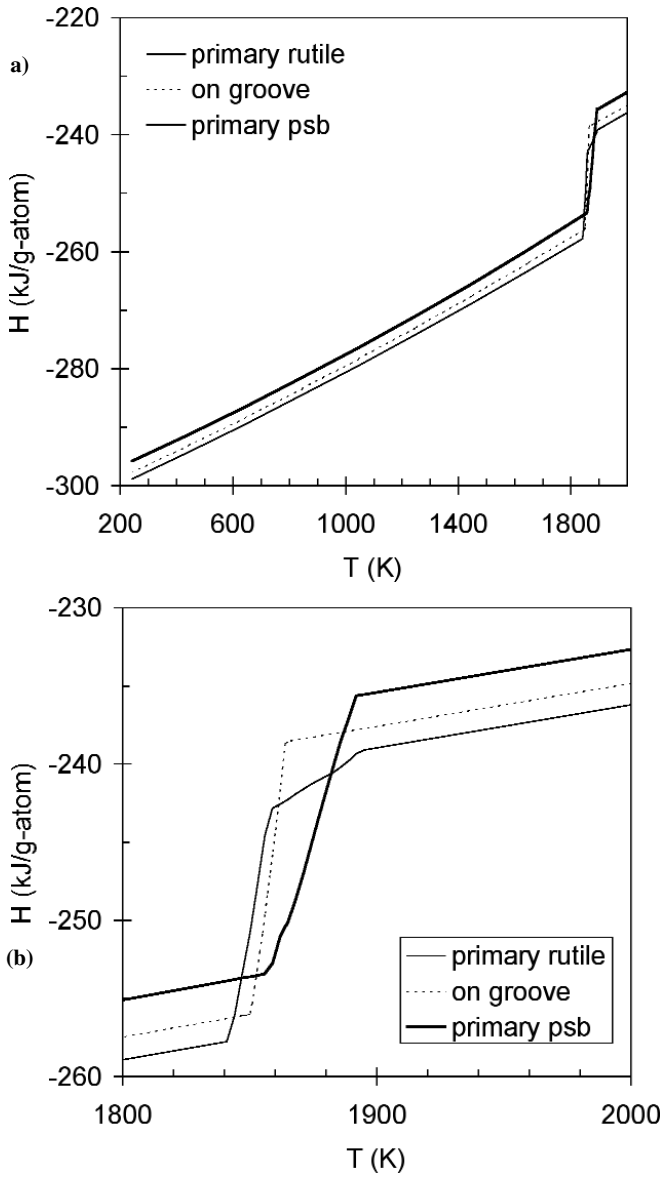

Figure 3. Change in enthalpy of mixtures containing an average of 10% FeO, for mixtures which, upon solidification, form respectively primary rutile (composition: X_{FeO} = 0.123, X_{TiO_2} = 0.73, $X_{Ti_2O_3}$ = 0.147), primary pseudobrookite ('psb') (X_{FeO} = 0.135, X_{TiO_2} = 0.58, $X_{Ti_2O_3}$ = 0.285), and both rutile and pseudobrookite simultaneously ('on groove') (X_{FeO} = 0.127, X_{TiO_2} = 0.674, $X_{Ti_2O_3}$ = 0.199). Results are shown over a wide temperature range (a), and in the vicinity of the liquidus and solidus temperatures (b)

The large vertical steps in the enthalpy plots, in the range 1840–1890K, indicate the solid-liquid transition. In each case, the transition occurs over a narrow temperature interval of–at most–30K. The heat of solidification is more than 17 kJ/g-atom in all three cases. Comparison with the heat capacity of the molten slag of 0.0275 kJ/g-atom (see Table II) reveals that solidification causes as large an enthalpy change as would a temperature change, in the case of fully liquid slag, of more than 600 K.

Heat transfer and energy balance model

An approximate one-dimensional pseudo-steady-state heat transfer calculation was used here; its main features are illustrated by Figure 4. The rate of heat transfer through the

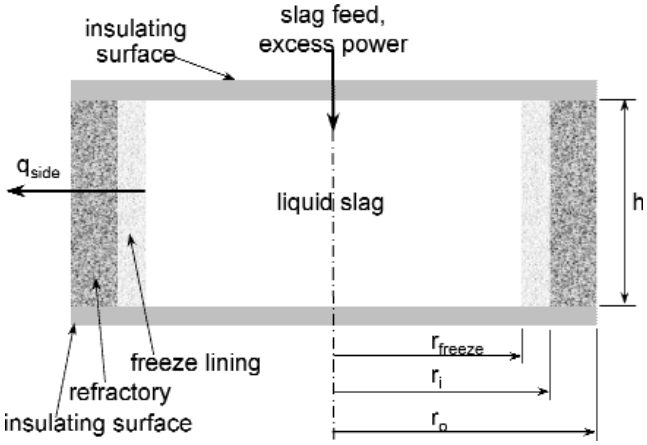

Figure 4. Schematic of the main features of the one-dimensional heat transfer model

furnace lining was calculated from the series resistances through the freeze lining and the furnace wall. In both cases, the resistance is calculated from the following relationship[6]:

$$R_{conduction} = \left[1n\left(r_{outer} / r_{inner}\right)\right] / (2\pi kh) \quad [1]$$

where r_{outer} and r_{inner} are the radii at the outside and inside of the conductor, k is its thermal conductivity, and h the height of the conductor (which is the depth of the slag bath; see Figure 4). It was assumed that the resistances at the outside of the furnace lining (i.e. through the steel shell, and conduction to the cooling water) are negligible. The rate of heat loss through the furnace wall is hence given by:

$$q_{side} = \left(T_{slag} - T_{water}\right) / \left(R_{freeze} + R_{refractory}\right) \quad [2]$$

where T_{slag} is the temperature of the slag and freeze lining in the furnace, T_{water} is the temperature of the cooling water, R_{freeze} is the conduction resistance through the freeze lining, and $R_{refractory}$ is the conduction resistance through the refractory.

Values of the constants used in this model are given in Table III. As these values show, the physical size of the modelled furnace corresponds to a pilot-scale furnace. This size of furnace was chosen for several reasons: the availability of data for this furnace,[7] the large wall contact area relative to slag volume (which will tend to emphasize any freeze lining effect), and the observation that the compositional relationships in these slags do not depend on furnace design[2] (i.e. any effect which controls the relationship between FeO and Ti_2O_3 must also apply to the pilot-scale furnace).

Table III
Constants used in heat transfer model.

Cooling water temperature (K)	303
Thermal conductivity of refractory (W/mK)	4.0
Thermal conductivity of freeze lining (W/mK)	1.0
Outer radius of refractory (m)	1.1
Inner radius of refractory (m)	0.9
Initial slag bath depth (m)	0.1
Molar density of slag and freeze (mol/m^3) (Species used are FeO, TiO_2 and Ti_2O_3)	4.0x10^4

Together with the conduction heat transfer calculation, the energy balance included the effects of feeding slag into the slag bath, and of applying power (by arcing) to the bath. The slag fed to the bath was specified by its molar flow rate, its composition, and its temperature. In specifying the feed to the bath as slag (rather than ilmenite and carbon), the details of the chemical reaction were not considered. The slag flow and current furnace contents were inputs to the mass balance: after each time interval, the amounts of FeO, TiO_2 and Ti_2O_3 in the furnace were recalculated, from the amount that had been in the furnace at the start of the time interval, and the amount that entered in the slag feed during the interval.

In performing this mass balance, no chemical reaction subsequent to the initial reduction of the ilmenite was assumed to take place (i.e. no redistribution of oxygen between iron and titanium was allowed). The energy balance was performed similarly, by finding the total enthalpy of the bath from the enthalpy of the slag bath at the start of each time interval, the enthalpy of the slag which was fed, heat lost through the furnace wall (Equation 2), and power input from the arc. From the energy balance and mass balance, the molar enthalpy and average composition of the furnace at the end of the time interval was known. This was then used to find the furnace temperature from the calculated dependence of enthalpy on temperature for the specific composition (i.e., using data such as shown in Figure 3). A simple interpolation procedure was used to determine temperature from enthalpy.

From the new furnace temperature and slag composition, the fraction of solid material was calculated (with the phase diagram information); this was then used to find the new thickness of the freeze lining. In this calculation, it was assumed that the molar densities of the freeze lining and liquid slag are equal (with the value as given in Table III). The new depth of the slag bath was similarly found from the mass balance (the total number of moles of material, whether solid or liquid, in the furnace), the internal diameter of the furnace, and the molar density.

This simplified approach neglects many of the complexities that arise in actual furnaces. Here, the freeze lining is assumed to be in full equilibrium with the liquid slag, with the possibility to change its composition within one time step. In reality, at most limited diffusion will occur within the solid lining. Also, temperature differences within the liquid slag are neglected, as are two-dimensional heat transfer (to the furnace roof above, and the metal bath below), and the details of chemical reaction kinetics. Most of these effects are incorporated in a much more detailed model which is being developed. However, this simplified model already offers useful insights, as discussed below.

Results and discussion

The results presented below refer to the pilot-scale furnace as discussed earlier. For this furnace, the typical maximum power input into the bath (excluding heat losses to the roof) is some 1 MW, with an ilmenite feeding rate of up to 1 ton/h. This typically resulted in the bath depth increasing by 0.3 m over 5 hours (corresponding to a slag mass increase of approximately 3 tons).

For each slag production rate and slag composition, the required power and reductant inputs were calculated from a simple mass and energy balance. In this calculation, it was assumed that the slag, CO, and liquid iron (with 2% C in solution) are produced at the stated feed temperature of the slag. The enthalpy data as listed in Table II were used for the liquid slag, with other values taken from literature compilations.[8,9], The feed material was assumed to be stoichiometric ilmenite ($FeTiO_3$) and pure carbon, at 298 K.

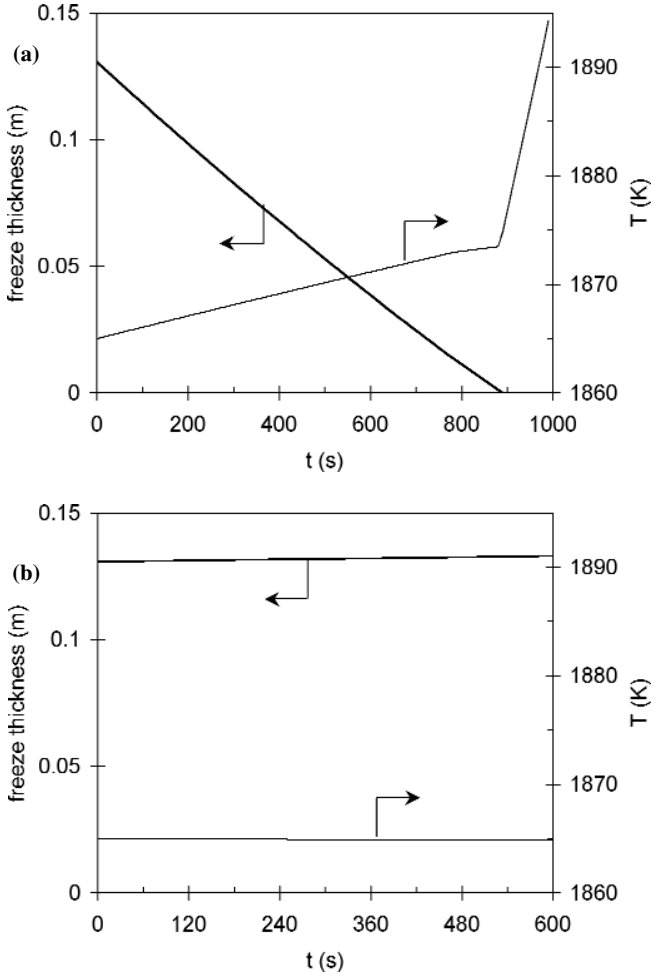

Figure 5. Calculated response of freeze lining thickness and furnace temperature, if no ilmenite is fed to the furnace. Furnace dimensions as given in Table III, and with slag depth (*h*) of 0.5 m, slag composition of X_{FeO} = 0.13, X_{TiO2} = 0.64, X_{Ti2O3} = 0.23, and initial furnace temperature of 1865 K. Calculated for (a) 1 MW of power input to the slag, and (b) zero power input

Freeze lining stability

In furnaces of this type, accurate control of the mass and energy balance is crucial, because producing the slag requires a specific balance of reductant and power input.[10] Disturbing this balance can cause loss (melting) of the freeze lining, or solidification of the furnace contents. Hence supplying electrical power without feeding ilmenite and reductant is inherently dangerous. This is illustrated by Figure 5, which shows the effect on the freeze lining thickness of maintaining the power input at 1 MW (without any feed), when the bath is 0.5 m deep. This calculation is for a thick initial freeze lining, of 0.13 m (solids fraction 27% of furnace contents).

Even with this thick lining, the lining is lost after 15 minutes of power input (beyond which time attack of the refractory lining will start). The effect of the heat of solidification to maintain the furnace temperature at a nearly constant value is also evident in Figure 5 (a); note the rapid heating once the freeze lining has been melted

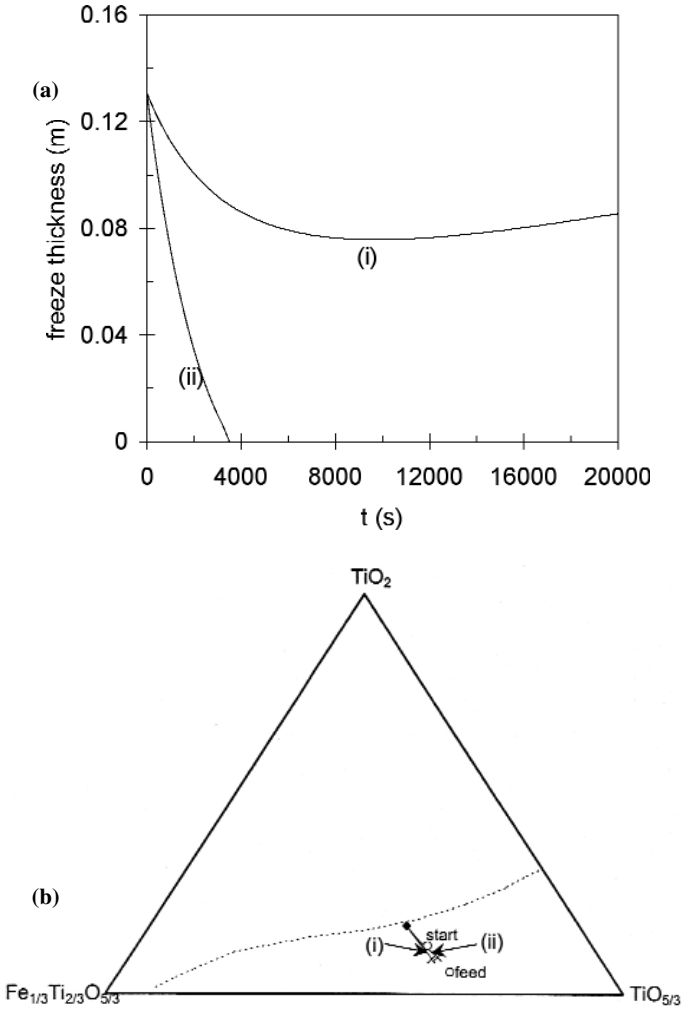

Figure 6. Effect of slag feeding and excess power on the liquid slag composition and freeze lining thickness, for the case where the freeze lining is pseudobrookite. Excess power: (i) zero, and (ii) 0.06 MW. (a) Change in freeze lining thickness, for the two levels of excess power. (b) Change in the composition of the liquid slag, where the initial composition of the material in the furnace is X_{FeO} = 0.13, X_{TiO_2} = 0.64, $X_{Ti_2O_3}$ = 0.23 (indicated by the label 'start' in the figure), at 1865 K, 0.1 m deep. Feed slag composition X_{FeO} = 0.13, X_{TiO_2} = 0.6, $X_{Ti_2O_3}$ = 0.27 (indicated by the label 'feed'), at 1895 K. Feed rate: equivalent to 1.08 t/h of ilmenite; 1.06 MW. The diamond gives the initial composition of the liquid slag, the lines the changes in the liquid slag compositions, and the crosses the compositions at the end of the simulation period (20 000 s in case [i], 4 500 s in case [ii])

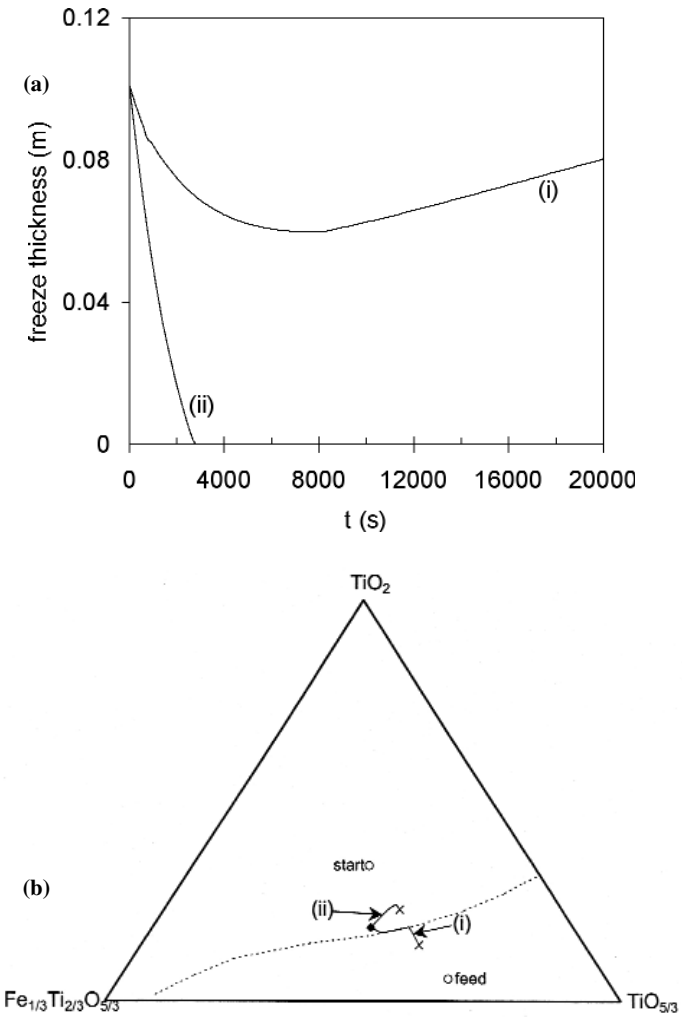

Figure 7. Effect of slag feeding and excess power on the liquid slag composition and freeze lining thickness, for the case where the freeze lining is rutile. Excess power: (i) zero, and (ii) 0.06 MW. (a) Change in freeze lining thickness, for the two levels of excess power. (b) Change in the composition of the liquid slag, where the initial composition of the material in the furnace is X_{FeO} = 0.121, X_{TiO_2} = 0.75, $X_{Ti_2O_3}$ = 0.129 (indicated by the label 'start' in the figure), at 1860 K, 0.1 m deep. Feed slag composition X_{FeO} = 0.13, X_{TiO_2} = 0.6, $X_{Ti_2O_3}$ = 0.27 (indicated by the label 'feed'), at 1895 K. Feed rate: equivalent to 1.08 t/h of ilmenite; 1.06 MW. The diamond gives the initial composition of the liquid slag, the lines the changes in the liquid slag compositions, and the crosses the compositions at the end of the simulation period (20 000 s in case [i], 3 300 s in case [ii])

away completely. Note also the very low rate at which the freeze lining grows (and the furnace contents cool down) if no power is input (Figure 5 b). This emphasizes that, while the freeze lining can be melted away rapidly, regrowth of the lining is a much slower process. (Slightly faster solidification than that shown in Figure 5 b will be found in practice, because of additional heat loss to the furnace roof and metal bath).

These effects can be understood in quantitative terms by noting that the heat of solidification of 17 kJ/g-atom is equivalent to 57 kJ/mol (where the slag species considered are FeO, TiO_2, and Ti_2O_3), or 2.3 GJ/m^3. With 27% of solids in the furnace, and a total bath depth of 0.5 m, the volume of solids is 0.34 m^3, which requires some 776 MJ to melt. If the total 1 MW of power input goes towards melting the freeze lining, total melting is hence expected to take only 776 s. The actual time is about 15% longer than this, reflecting the comparatively small effect of heat losses through the furnace lining: with no freeze lining, the heat loss by conduction through the furnace wall (per unit depth of slag) is some 200 kW/m.

In contrast with this, if the freeze lining is 0.13 m thick, the rate of heat loss through the furnace wall is only some 48 kW/m, corresponding to a rate of solidification of the lining of some 15 mm/h.

Slag composition response to inputs

The suggestion that is tested here is that solidification equilibrium with the freeze lining forces the slag composition to lie along the eutectic groove. The suggestion was evaluated by varying the starting compositions, initial freeze lining thickness, slag feed, slag

temperature, and excess power. Two representative sets of results are shown in Figures 6 and 7. In both cases, the furnace contained material with 10% FeO by mass, but in the case of Figure 6 the starting composition lay between M_3O_5 and the eutectic groove, and for Figure 7 the starting composition was between the eutectic groove and rutile. In both cases, the starting temperature was selected to yield a liquid slag composition, which was close to the eutectic groove; this liquid was in contact with a pseudobrookite freeze lining for the conditions of Figure 6, and with a rutile freeze lining for Figure 7. In both cases, the feed slag was chosen to contain 10% FeO, but with less TiO_2 (and hence more Ti_2O_3) than both starting compositions.

Two sets of results are shown for each combination, which are for different levels of excess power: zero, and 0.06 MW. The latter represents an excess of some 6%. While an apparently small percentage, this in fact is a large excess power, equivalent to superheating the liquid slag feed by nearly 400 K.

It is apparent from the results that the solidification equilibrium does *not* constrain the slag to the eutectic groove. In the first case (Figure 6), where both the starting and feed compositions lie between M_3O_5 and the eutectic groove, the liquid slag composition changes *away from* the eutectic groove, towards the feed composition; this happens whether the freeze lining remains at approximately the same thickness (case [i]), or is melted away as a result of the excess power (case [ii]).

Where the starting and feed slag compositions are on opposite sides of the eutectic groove (Figure 7), the liquid slag composition does follow the eutectic groove for some time, for the case of zero excess power (i.e. where the freeze lining is not melted away, case [i]). However, in this case and as before, the liquid slag composition eventually departs from the eutectic groove, and changes towards the feed composition.

The conclusion from these and several other simulations (not shown here because of space limitations) is that, in contrast with the suggestion that the freeze lining can affect slag composition, the influence works in the opposite direction: changes to the inputs into the slag bath (slag composition and power) have a direct effect on the freeze lining. This result emphasizes the importance of close control of the furnace inputs, to ensure stability.

Conclusions

From this simple heat transfer model and slag solidification equilibria, it appears that the phase equilibrium between liquid slag and freeze lining cannot serve to constrain the liquid slag composition to the eutectic groove. (This conclusion is being tested with a more complete model.) The question remains what mechanism is responsible for the very consistent compositional relationship between the FeO and Ti_2O_3 contents in titania slags.

In previous work it was shown that this relationship does not follow from the reaction equilibrium (between Fe, FeO, TiO_2, and Ti_2O_3)[11] ; in the work presented here, it seems that it is not a result of the solidification equilibrium either. From the present work, it is clear that the composition of newly reduced slag, which enters the slag bath plays a dominant role, and that this role is largely undiminished by interaction with the freeze lining. The composition of the feed slag depends on the ratio of reductant to ilmenite, but also on the relative extents of reduction of FeO (to Fe), and of TiO_2 (to Ti_2O_3).

The conclusion hence is that the inherent kinetics of these parallel reduction reactions is the likely origin of the observed slag composition relationship. Another factor is that the compositional range where the slag is fully liquid is not large, at typical operating temperatures (Figure 2), with the result that liquid slag compositions cannot depart much from M_3O_5 stoichiometry.

Acknowledgement

I am grateful for useful discussions with Hanlie du Plooy and Johan Zietsman. The research was made possible by support by Kumba Resources, and the Technology and Human Resources for Industry Programme (THRIP) managed by the National Research Foundation (NRF) and financed by the dti. This material is based on work supported by the National Research Foundation under grant number 2053355.

References

1. PISTORIUS, P.C. Physicochemical aspects of titanium slag production and processing. *Proceedings, Mills Symposium, Metals, Slags, Glasses*: *High Temperature Properties & Phenomena*, London, Aune, R.E. and Sridhar, S. (eds.). Teddington, United Kingdom. National Physical Laboratory, 2002. vol. 1, pp. 273–281. An updated version of this paper will appear as: Pistorius, P.C., and Coetzee, C. Physicochemical aspects of titanium slag production and solidification. *Metallurgical and Materials Transactions Series B*, in press.
2. PISTORIUS, P.C. The relationship between FeO and Ti_2O_3 in ilmenite smelter slags. *Scandinavian Journal of Metallurgy*, vol. 31, no.2. 2002. pp. 120-125.
3. BALE, C.W., CHARTRAND, P., DEGTEROV, S.A., ERIKSSON, G., HACK, K. BEN MAHFOUD, R., MELANÇON, J., PELTON, A.D., and PETERSEN, S. FactSage Thermochemical Software and Databases. *CALPHAD*, vol. 26, no. 2. 2002. pp.189–228.
4. ERIKSSON, G., PELTON, A.D., WOERMANN, E. and ENDER, A. Measurement and thermodynamic evaluation of phase equilibria in the Fe-Ti-O system. *Ber. Busenges. Phys. Chem.*, vol. 100, no. 11. 1996. pp. 1839-1849.
5. TURKDOGAN, E.T. *Physicochemical properties of molten slags and glasses*. London, The Metals Society, 1983. pp. 125-139.
6. HAHNE, E. and GRIGULL, U. Formfaktor und Formwiderstand der stationären mehrdimensionalen Wärmeleitung. *Int. J. Heat Mass Transfer*, vol. 18. 1975. pp. 751-767.
7. BESSINGER, D., DU PLOOY, H., PISTORIUS, P.C., and VISSER, C. Characteristics of some high titania slags. *Heavy Minerals 1997*. Robinson, R.E. (ed.). Johannesburg. The South African Institute of Mining and Metallurgy, 1997. pp. 151-156.
8. KUBASCHEWSKI, O., ALCOCK, C.B. and SPENCER, P.J. *Materials thermochemistry*, 6th edition. Oxford, Pergamon. 1993. pp. 258-323.
9. RIST, A. and CHIPMAN, J. L'activité du carbone dissous dans le fer liquide. *Revue de Métallurgie*, vol. 53, no. 10. 1956. pp. 796-807.
10 PISTORIUS, P.C. Limits on energy and reductant inputs in the control of ilmenite smelters. *Heavy Minerals 1999*. Stimson, R.G. (ed.). Johannesburg. The South African Institute of Mining and Metallurgy, 1999. pp. 183-188.
11. GELDENHUIS, J.M.A. and PISTORIUS, P.C. The use of commercial oxygen probes during the production of high titania slags. *Journal of the South African Institute of Mining and Metallurgy*, vol. 99, no. 1. 1999. pp. 41-47.